Free-Field Correction Factor for Spherical Acoustic Waves Impinging on Cylinders

C. R. Fuller*
Virginia Polytechnic Institute and State University, Blacksburg, Virginia

The scattering and diffraction of spherical waves by an infinite rigid cylinder is analytically studied for monopole and dipole acoustic sources. A correction factor at the cylinder surface for the change in the free-field radiation levels due to the presence of the cylinder is calculated. The results indicate that the correction factor is sensitive to source frequency and location. Regions of negative correction factor due to shadowing and creeping wave behavior are identified. The analysis is applied to a simplified representation of propeller lift noise and the correction factor in the shadowed region is demonstrated to be strongly dependent on blade angle.

Nomenclature

a = cylinder radius
A_n = scattered spectral amplitude
c = speed of sound
I_1, I_2 = integrand functions
k_r = radial wavenumber
k_n = axial wavenumber
k_0 = free wavenumber
n = circumferential modal number
p_i = free-field pressure
P_s = scattered preessure
p_t = total pressure
p_0 = source amplitude (force/length)
r, θ, x = cylindrical coordinates
R_s = source radial location
γ = propeller blade angle
α_c = scattering correction factor
ϵ_n = 1, $n = 0$; = 2, $n > 0$
ω = frequency (rads/s)
$(')$ = derivative with respect to r

Introduction

INTERIOR noise in aircraft has recently received much attention.[1] The main impetus for these works has been the imminent advent of the advanced turbo propeller (ATP) which, although being fuel efficient, is also an extremely loud acoustic source. Research into cabin noise prediction has been split into several areas.[1] Much work has been done in predicting sound levels from ATP's.[2] These predictions (e.g., the ANOPP code) subsequently have been used as the exterior acoustic forcing functions for analytical models designed to estimate the interior sound levels of representative aircraft.[3] However, the ANOPP code predicts the free-field pressure distributions of high-speed propellers and does not include scattering effects from nearby surfaces such as the fuselage. Thus, e.g., in Ref. 3, the acoustic pressures on the model aircraft fuselage are approximated by an empirically based formula.

Presented as Paper 87-2735 at the AIAA 11th Aeroacoustics Conference, Sunnyvale, CA, Oct. 19-21, 1987; received April 4, 1988; revision received Feb. 14, 1989.

*Professor of Mechanical Engineering. Member AIAA.

Although using this type of approximate approach to derive the correct exterior acoustic forcing functions appears to give reasonable results, it would be a significant improvement to interior noise prediction to be able to calculate a more representative correction factor for the presence of the fuselage. Similarly, such an investigation would have the necessary formulations to calculate the effect of a scattering surface on far-field radiation patterns.

In this paper, the effect of the presence of an infinite rigid cylinder on the free-field radiation of monopole and dipole sources of various orientations is considered. The investigation is a fundamental step toward understanding radiation from more complex sources, such as propellers, in the presence of scattering surfaces as these can be considered to be constructed from sets of distributed monopoles, dipoles, etc. of appropriate strengths, phases, and orientations.[4]

The problem is formulated in various stages and generally follows the analysis of James,[5] who considered the effect of a cylinder of finite surface impedance on the far-field radiation of a monopole. Previously, Uberall et al.[6] analytically studied the scattering of plane acoustic waves incident upon a soft infinite cylinder. Junger[7] has also considered the radiation of sound from a piston set in a sphere and a strip on the surface of an infinite rigid cylinder. Both of these works used the Sommerfeld-Watson transformation to reduce the wave-harmonic series to a manageable form when $k_0 a$ is large. One of the interesting outcomes of Uberall's and Junger's work was the identification of "creeping waves" due to diffracted waves traveling in angular directions around the scattering object. Recently, SenGupta[8] has numerically evaluated the scattering correction factor for a point source located near a rigid cylinder. His results show good agreement with experiments. When the point source is replaced with a line source, good agreement is also demonstrated between numerical and closed-form solutions of the type to be used here.

Figure 1 shows the geometry of the situation. First, the radiation from a monopole source is transformed to cylindrical coordinates. Second, a scattered field from the cylinder surface is assumed and the amplitudes of the scattered waves are calculated by application of the appropriate boundary condition at the cylinder surface. Thus, on obtaining the scattered-wave amplitudes, the ratio of the free-field acoustic pressure to the total acoustic pressure at the cylinder surface can be calculated.

Analysis

The free-field pressure distribution radiated by a monopole source located at $r = R_s$, $\theta = 0$, $x = 0$, can be expanded into

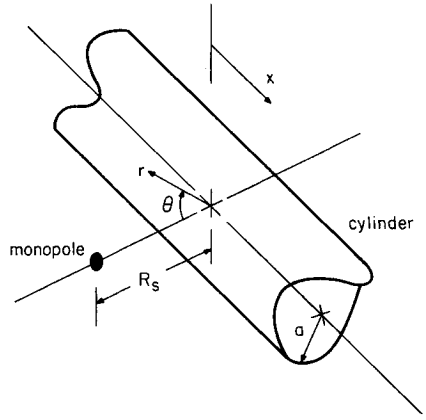

Fig. 1 Geometry and coordinate system.

cylindrical coordinates using a Fourier transform and a special case of the Bessel function addition theorem as[5,9]

$$p_i(r,\theta,x,R_s) = \frac{ip_0}{2}\sum_{n=0}^{\infty}\epsilon_n\cos(n\theta) \times \int_{-\infty}^{\infty} J_n(k_r r)H_n(k_r R_s)\exp[ik_n x]\,dk_n \qquad \text{for } r<R_s \quad (1)$$

where $k_n^2 = k_0^2 - k_r^2$ and the free wavenumber $k_0 = \omega/c$. If the monopole source is positioned near an infinite rigid cylinder, the free-field pressure term must be argumented by a scattering term for reflections from the cylinder surface. The total pressure field in the presence of the cylinder can be written as

$$p_t = p_i + p_s \quad (2)$$

where the scattered field has the form of[10]

$$p_s(r,\theta,x = \frac{1}{\sqrt{2\pi}}\sum_{n=0}^{\infty}\cos(n\theta) \times \int_{-\infty}^{\infty} A_n(k_n)H_n(k_r r)\exp[ik_n x]\,dk_n \quad (3)$$

Application of the boundary condition of continuity of normal displacement at the cylinder surface, $r = a$, gives, for a rigid cylinder,

$$\left.\frac{\partial p}{\partial r}\right|_{r=a} = 0 \quad (4)$$

Thus, substituting Eqs. (1) and (3) into Eq. (2) and performing the derivative gives

$$\frac{ip_0}{2}\sum_{n=0}^{\infty}\epsilon_n\cos(n\theta)\int_{-\infty}^{\infty}J_n'(k_r a)H_n(k_s R_s)\exp[ik_n x]\,dk_n + \frac{1}{\sqrt{2\pi}}\sum_{n=0}^{\infty}\cos(n\theta)\int_{-\infty}^{\infty}A_n(k_n)k_r H_n'(k_r a)\exp[ik_n x]\,dk_n = 0 \quad \text{at} \quad r = a \quad (5)$$

Rearranging this equation to solve for the unknown spectral amplitude of the scattered waves A_n gives

$$A_n(k_n) = -\frac{i\sqrt{2\pi}\,p_0}{2}\epsilon_n\frac{J_n'(k_r a)H_n(k_r R_s)}{H_n'(k_r a)} \quad (6)$$

Resubstituting the relation for $A_n(k_n)$ into Eqs. (3) and (2) gives the total pressure as

$$P_t(r,\theta,R_s,x) = \frac{ip_0}{2}\sum_{n=0}^{\infty}\epsilon_n\cos(n\theta)\int_{-\infty}^{\infty}J_n(k_r r)H_n(k_r R_s) \times \exp[ik_n x]\,dk_n - \frac{ip_0}{2}\sum_{n=0}^{\infty}\epsilon_n\cos(n\theta)\int_{-\infty}^{\infty}\frac{J_n'(k_r a)H_n(k_r R_s)}{H_n'(k_r a)} \times H_n(k_r r)\exp[ik_n x]\,dk_n \quad \text{for } r<R_s \quad (7)$$

The calculate a correction factor in decibels between the free-field pressure and the total pressure (blocked) at the cylinder surface, we need to calculate both p_i and p_t at $r = a$ and form the ratio as

$$\left.p_t/p_i\right|_{r=a} = 1 + p_s/p_i \quad (8)$$

Thus,

$$\left.p_t/p_i\right|_{r=a} = 1 - \frac{\sum_{n=0}^{\infty}\epsilon_n\cos(n\theta)I_1}{\sum_{n=0}^{\infty}\epsilon_n\cos(n\theta)I_2} \quad (9)$$

where the integrands are specified by

$$I_1(k_n,k_0,x,R_s) = \int_{-\infty}^{\infty}\frac{J_n'(k_r a)H_n(k_r R_s)}{H_n'(k_r a)}H_n(k_r a)\exp[ik_n x]\,d(k_n a) \quad (10)$$

$$I_2(k_n,k_0,x,R_s) = \int_{-\infty}^{\infty}J_n(k_r a)H_n(k_r R_s)\exp[ik_n x]\,d(k_n a) \quad (11)$$

Equation (9) can be easily expanded using superposition principles for a dipole-type source consisting of two out-of-phase monopoles as

$$\left.p_t/p_i\right|_{r=a} = 1 - \frac{\sum_{s=1}^{2}(-1)^{s+1}\sum_{n=0}^{\infty}\epsilon_n\cos(n\theta)I_1}{\sum_{s=1}^{2}(-1)^{s+1}\sum_{n=0}^{\infty}\epsilon_n\cos(n\theta)I_2} \quad (12)$$

where the index s corresponds to the two components of the dipole. The scattering correction factor can then be calculated from

$$\alpha_c = 20\log_{10}\left(\left.p_t/p_i\right|_{r=a}\right) \quad (13)$$

Results and Discussion

In order to evaluate the correction factor of Eq. (12), it is necessary to evaluate the integrals numerically. This was done using Simpson's rule implemented on a Cyber computer. Likewise, it is necessary to truncate the modal sums of Eq. (12). As values of $k_0 a$ considered were reasonably low, a wave-harmonic series approach was possible. In this case, the correction factor was found to converge to sufficient accuracy with 20 circumferential modes included, i.e., $n = 19$. Differing nondimensional frequencies, source, and evaluation locations were considered in order to uncover the scattering mechanisms. The range of variation of the parameters was chosen to include those that might correspond to a typical ATP application, i.e. $k_0 a \approx 4.0$ and $R_s/a \approx 2.0$. Most of the evaluations are presented for $0 \le \theta \le 180$ deg as the plots are symmetrical about the source plane. Figures 2, 4, and 5 are for a monopole source, while Figs. 6 and 7 compare monopole and dipole radiation. For the dipole, two sources of equal amplitude and

opposite phase are included with a radial spacing of $\Delta R_s/a = 0.1$.

Figure 2 gives the correction factor for a nondimensional axial and radial source location of $x/a = 0$, $R_s/a = 2.0$, respectively. The nondimensional driving frequency is varied from $k_0a = 0.5$ to 4.0. The scattering correction factor can be seen to be strongly dependent upon frequency. At low frequencies where the wavelength is much longer than the cylinder diameter, the correction factor at $\theta = 0$ is of the order of +3.5 dB. With increasing frequency, the correction factor at $\theta = 0$ steadily approaches the expected value of a normal incidence wave of 6 dB.

Similarly, as the source frequency is increased, the correction factor in the "shadowed" surface of the cylinder is reduced. At long wavelengths relative to cylinder diameter, most of the acoustic energy is simply diffracted around the cylinder and the correction factor is negative but small. At shorter wavelengths, the cylinder tends to"shadow" the region on its trailing side, and thus the free-field pressure value is much greater than the total pressure in this region with the cylinder present.

Interestingly, the minimum correction factor for all cases occurs at locations other than $\theta = 180$ deg. This behavior was thought to be due to "creeping waves" traveling around the surface as previously observed in Refs. 5 and 6. When an acoustic wave impinges on a closed body of revolution, there are two main effects, as illustrated in Fig. 3. First, there is direct scattering due to direct reflection of the incidence wave front from the surface. Second, the waves are diffracted around the cylinder surface and travel circumferentially in opposite directions. Thus, at some locations, the waves traveling in opposite directions, called creeping waves, interfere destructively, resulting in a larger negative correction factor.

In Fig. 4, the effect of a variation in source location for $k_0a = 4.0$ and $x/a = 0$ is given. At $\theta = 0$, the correction factor for all cases is 5.5 dB. Moving the source away from the cylinder can be seen to increase the correction factor in the region $0 \leq \theta \leq 90$ deg due to the effective wave front incidence angle decreasing (relative to a normal to the cylinder surface) as the source location increases. Similarly, in the region of 90 deg $\leq \theta \leq 180$ deg the correction factor increases with source radial location. Decreasing the angle of incidence of the wave front a cylindrical surface causes increased reflection of the wave front off the surface and less diffraction, as there is more projected cylinder surface area normal to the wave front. However, the illuminated area of the cylinder surface increases with source location as well, and this tends to increase the levels on the trailing side of the cylinder.

The influence of location of the axial evaluation point is studied in the results of Fig. 5, where $k_0a = 4.0$ and $R_s/a = 2.0$. Generally, for the range of $0 < x/a \lesssim 2.0$, the results are insensitive to axial location. For $x/a \gtrsim 2.0$, the correction factor gradually decreases as x/a increases, again due to the angle of incidence of the wave front increasing with axial distance. Likewise, on the trailing side of the cylinder, the correction factor is insensitive to axial location for $0 < x/a \lesssim 2.0$. For $x/a \gtrsim 2.0$, the amplitudes on the trailing side gradually increase as more diffraction of waves around the cylinder surface occurs due to increasing angle of incidence of the wave front.

Finally, Figs. 6 and 7 compare correction factors for a monopole and dipole source located at $R_s/a = 1.1$ and 4, respectively. In this case, the dipole is orientated with its minor axis along a radius. In both figures, $k_0a = 4.0$ and $x/a = 0$. When the source is close to the cylinder surface, there are significant differences between the correction factors of a monopole and a dipole. It is apparent in Fig, 6 that while the correction factor at $\theta = 0$ is unchanged, at other angular locations there is a significant difference. For the region $0 < \theta \lesssim 90$ deg, the monopole correction factor is greater than the dipole.

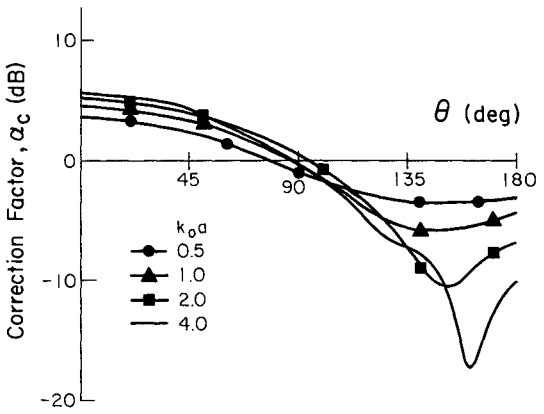

Fig. 2 Correction factor, monopole source, $x/a = 0$, $R_s/a = 2.0$.

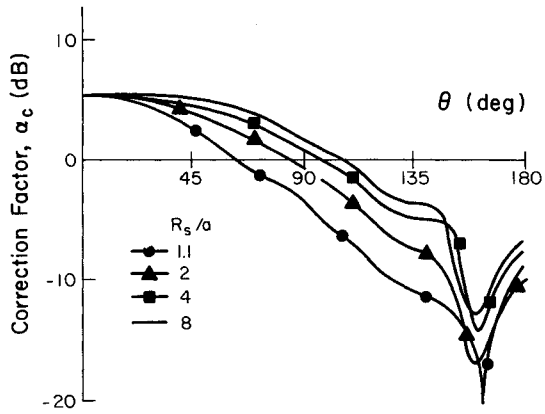

Fig. 4 Correction factor, monopole source, $k_0a = 4.0$, $x/a = 0$.

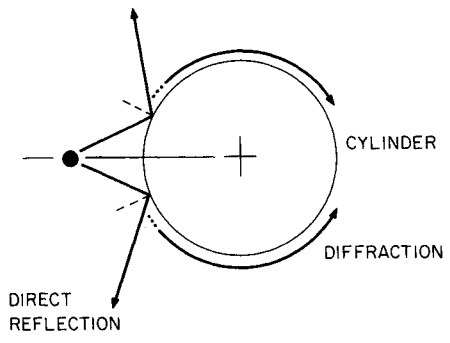

Fig. 3 Cylinder scattering mechanisms.

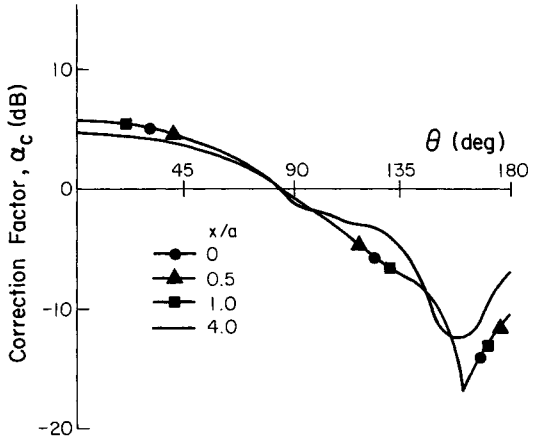

Fig. 5 Correction factor, monopole source, $k_0a = 4.0$, $R_s/a = 2.0$

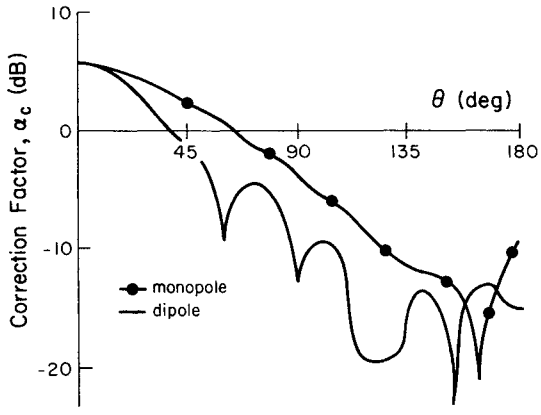

Fig. 6 Correction factor, $k_0a = 4.0$, $R_s/a = 1.1$, $x/a = 0$.

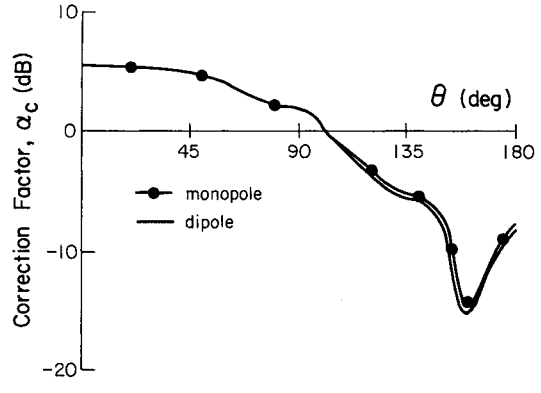

Fig. 7 Correction factor, $k_0a = 4.0$, $R_s/a = 4.0$, $x/a = 0$.

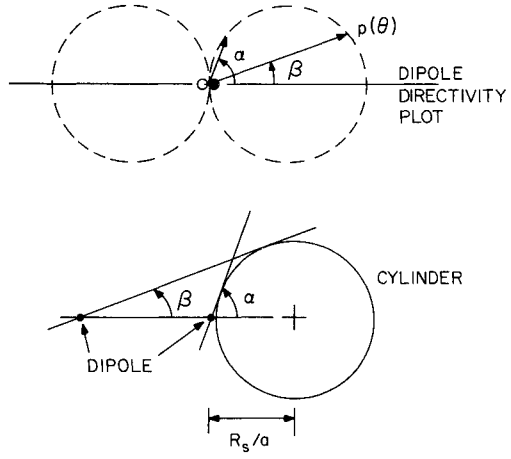

Fig. 8 Dipole geometry and radiation directivity pattern.

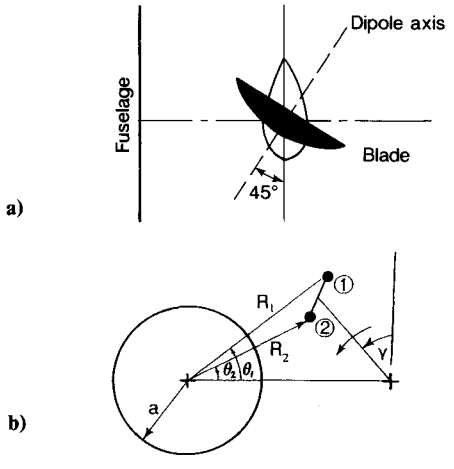

Fig. 9 Arrangement and coordinate system of rotating blade and dipole: a) top view, b) front view.

The behavior can be understood with the aid of Fig. 8. The effect is undoubtedly due to the highly directional nature of the dipole source which will have large subtended radiation angles when located near the cylinder surface and thus tend to radiate most of its energy towards $\theta = 0$, as demonstrated in Fig. 8. Hence, the dipole free-field pressure will be less affected on the front side of the cylinder. Similarly, the directional nature of the dipole source can be seen to cause some increased shadowing on the trailing side of the cylinder, 90 deg $\lesssim \theta \leq 180$ deg.

Again, peculiar oscillations in the correction factor curves are observed for 90 deg $\lesssim \theta \leq 180$ deg and are thought to be due to the aforementioned creeping waves. In particular, the correction curve for the dipole at $R_s/a = 1.1$ shows marked oscillations. This is probably due to the overall pressure amplitude being small, and thus the presence of the creeping waves is readily apparent.

When the source is located at $R_s/a = 4.0$, well away from the cylinder, there is little difference between the results of the dipole and the monopole, as demonstrated in Fig. 7. This result is most likely due to the subtended radiation angles of the dipole source being small in this case, as shown in Fig. 8, and thus directivity plays little role.

Application to Propeller Noise

It is of interest to aeroacousticians to apply the analysis to propeller noise. As a simple approximation, the lift component of propeller noise can be modeled as a dipole[4] positioned as in Fig. 9a. For this case, it is assumed that the noise source is due to a single blade orientated at 45 deg to the x axis. As the blade rotates, the dipole changes it position and orientation as depicted in Fig. 9b. Thus, for various angles of the blade relative to the vertical, the installation correction factor of the cylinder (representative of a fuselage) can be calculated. It should be noted that the analysis does not include various important characteristics such as translation of the dipole and convection of the propagating medium. However, it is expected that the results will still shed light on an area that has received little attention in propeller noise, and the added complexity could be the topic of further work.

Figure 10 gives the correction factors calculated for three blade angles, $\gamma = 0$, 45, and 90 deg. For these cases, the source frequency and location (at $\gamma = 90$ deg) is again assumed to be $k_0a = 4.0$ and $R_s/a = 2.0$. The coordinates of the source components calculated from Fig. 9b are given in Table 1.

When the blade is vertical, $\gamma = 0$ deg, the maximum correction factor occurs near $\theta \simeq 10$ deg on a line directly toward the dipole for reasons discussed previously. As the observation angle θ increases, the correction factor decreases until on the backside of the cylinder, near $\theta = 180$ deg, substantial shadowing effects are indicated by a large negative correction factor. Oscillations in the curves in these regions are again thought to be associated with creeping wave behavior. Rotating the blade to $\gamma = 45$ deg causes little change in the curve except that the locations of the minimum are shifted somewhat due to differing dipole source orientation affecting the phase of the creeping waves.

When the blade is positioned at $\gamma = 90$ deg, or horizontally, the results are significantly different. The maximum correction factor on the illuminated side is still around 5 dB but has moved location to near $\theta = 0$ deg. However, on the backside of the cylinder near $\theta = 180$ deg, the correction factor is positive

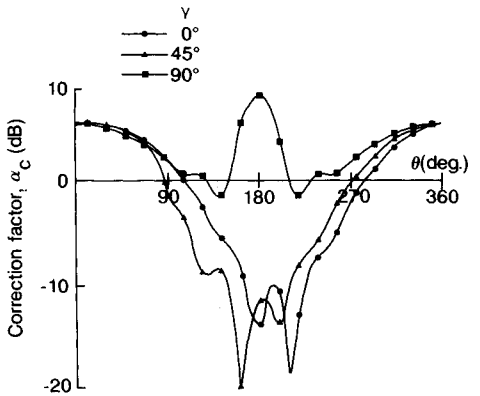

Fig. 10 Correction factor, $k_0a = 4.0$, $x/a = 0$.

Table 1 Coordinate location of dipole vs blade angle

	$\gamma = 0$		$\gamma = 45$ deg		$\gamma = 90$ deg	
Source	1	2	1	2	1	2
R_s/a	2.787	2.719	2.288	2.205	2.0	2.0
x/a	−0.0353	0.0353	−0.0353	0.0353	−0.0353	0.0353
θ, deg	13.91	14.27	12.81	11.45	1.01	−1.01

and around 8 dB. A limit study confirmed that the correction factor at $\theta = 0$ and 180 deg does converge to the values mentioned even though p_i is zero at both locations in this case. These results imply that the presence of the cylinder has led to a large increase in the free-field levels at this blade orientation. As discussed previously, the reason for this behavior is largely due to the fact that at $\gamma = 90$ deg the dipole is much closer to the cylinder surface, resulting in a large increase in the diffraction of the waves around the cylinder, ultimately causing large increases in pressure amplitude.

Conclusions

The scattering and diffraction of spherical waves impinging on a rigid infinite cylinder have been analytically studied. Both a monopole and a dipole acoustic source have been considered. A correction factor at the cylinder surface has been calculated for the presence of the cylinder in the source free-field pressure radiation distribution. The results indicate that the correction factor is sensitive to source frequency and location and relatively insensitive to axial location of observation point. When the source is well away from the cylinder, there is little difference in the correction factor for a monopole or dipole source. However, when the source is very close to the cylinder, the directional nature of the dipole source causes significant differences.

Regions of negative correction factors on the trailing side of the cylinder were shown and are associated with acoustic shadowing of the cylinder. Oscillations in the correction curves with circumferential angle were found and are thought to be due to creeping waves traveling circumferentially around the cylinder.

Application of the analysis to a simplified situation representative of propeller "lift" noise shows that the blade angle has little effect on the correction factor for the illuminated side of the fuselage cylinder. However, on the shadowed side, the correction factor is strongly affected by blade angle, primarily due to the noise source near field impinging on the fuselage as it approaches the scattering surface. This result underlines the importance of considering a closed body of revolution as an acoustic scatterer representative of an aircraft fuselage.

Acknowledgments

The author is grateful to NASA Langley for their support of this research under Grant NAG1-390 and to Dr. S. Glegg of Florida Atlantic University for helpful comments.

References

[1]Mixson, J. S. and Powell, C. A., "Review of Recent Research on Interior Noise of Propeller Aircraft," AIAA Paper 84-2349, Sept. 1984.

[2]Farassat, F., "The Prediction of the Noise of Supersonic Propellers in Time Domain—New Theoretical Results," AIAA Paper 83-0743, Jan. 1983.

[3]Pope, L. D., Wilby, E. G., and Wilby, J. F., "Propeller Aircraft Interior Noise Model," NASA CR 3813, Aug. 1984.

[4]Gutin, L., "On the Sound of a Rotating Airscrew," NACA TM 1195, 1948 (translated from Russian in *Zhurnal Teknichesqoi Fizik,* Vol. 6, Jan. 1936, pp. 899–804).

[5]James, J. H., "Far-Field Sound Radiation of Point Source Near Locally Reacting Cylinder," AMTE Tech. Memo. TM81036, 1981.

[6]Uberall, H., Doolittle, R. D., and McNicholas, J. V., "Use of Sound Pulses for a Study of Circumferential Waves," *Journal of the Acoustical Society of America,* Vol. 39 No. 3, 1986, pp. 564–578.

[7]Junger, M. C., "Surface Pressures Generated by Pistons on Large Spherical and Cylindrical Baffles," *Journal of Acoustical Society of America,* Vol. 41, No. 5, 1967, pp. 1336–1346.

[8]SenGupta, G., "Computation of Aeroacoustic Scattering Effects," AIAA Paper 87-2669, Sept. 1987.

[9]Skelton, E. A., "Free-Space Green's Functions of the Reduced Wave Equation," AMTE Tech. Memo. TM82073, May 1982.

[10]Junger, J. C. and Feit, D., *Sound, Structures and Their Interaction,* MIT Press, Cambridge, MA, 1986.